

Direct and inverse superspin Hall effect in two-dimensional systems: Electrical detection of spin supercurrents

Vetle Risinggård* and Jacob Linder

Center for Quantum Spintronics, Department of Physics, NTNU,
Norwegian University of Science and Technology, N-7491 Trondheim, Norway
(Dated: April 11, 2019)

A useful experimental signature of the ordinary spin Hall effect is the spin accumulation it produces at the sample edges. The superspin Hall current [Phys. Rev. B **96**, 094512 (2017)] is a transverse equilibrium spin current which is induced by a charge supercurrent. We study the superspin Hall current numerically, and find that it does not give rise to a similar edge magnetization. We also predict and numerically confirm the existence of the inverse superspin Hall effect, which produces a transverse charge supercurrent in response to an equilibrium spin current. We verify the existence of the inverse superspin Hall effect both for a spin-polarized charge supercurrent and an exchange spin current, and propose that a ϕ_0 junction produced by the inverse superspin Hall effect can be used to directly and electrically measure the spin polarization of a charge supercurrent. This provides a possible way to solve the long-standing problem of how to directly detect the spin-polarization of supercurrents carried by triplet Cooper pairs.

I. INTRODUCTION

Spin-polarized supercurrents are a central theme in superconducting spintronics [1]. Cooper pairs in conventional Bardeen–Cooper–Schrieffer superconductors are in the spin-singlet state [2–4]. Consequently, supercurrents in conventional superconductors are not spin polarized. To spin polarize such a supercurrent, the spin-singlet pairs must be converted to equal-spin triplet pairs. This can be accomplished by combining the processes known as spin mixing and spin rotation [1, 5–7]. Because of the exchange splitting, proximity-induced Cooper pairs in a ferromagnet will oscillate between the spin-singlet and the spin-0 triplet state [8, 9]. This is known as spin mixing. A magnetic inhomogeneity or spin–orbit coupling can rotate the resulting spin-0 triplets into equal-spin triplets [10–14]. This is known as spin rotation. So far, such a spin polarization of the supercurrent carried by triplet Cooper pairs has not been detected directly, but is only inferred from otherwise inexplicably long-ranged supercurrents in proximity structures [7].

Long-ranged spin-polarized supercurrents in phase-biased Josephson junctions are equilibrium currents. Various authors have suggested that spin supercurrents have observable consequences that can be detected via electrical [15–17] or mechanical [18] means, or through the magnetization dynamics they induce [19, 20]. Nonetheless, experimental detection schemes based on these signatures have yet to be implemented. One particular difficulty with these suggestions is that an equilibrium spin current by definition cannot perform work without dissipating. Consequently, any attempt to extract useful work from, say, a voltage induced by an equilibrium spin current in order to detect that current will dissipate the spin current itself.

The spin Hall effect [21] and its Onsager reciprocal [22–24] have found many applications in nonsuperconducting spintronics. Among others, these include electrical detection of spin currents induced by spin pumping [25] or the spin Seebeck effect [26]; spin Hall magnetoresistance [27, 28]; and spin Hall

spin-transfer torques [29]. It is only natural to inquire whether a superconducting analog of the spin Hall effect can be used to detect the spin-polarization of a supercurrent.

Spin Hall effects in superconducting structures have been considered previously in several theoretical and experimental works. Refs. [30–35] considered out-of-equilibrium situations, in which quasiparticle effects give rise to spin (charge) currents as a result of charge (spin) injection. In particular, Ref. [35] measured an enhancement of the inverse spin Hall signal by three orders of magnitude when the NbN is cooled below the superconducting transition temperature. Refs. [36–40] considered equilibrium situations and it was shown that the combination of spin–orbit coupling and an exchange field could induce a phase difference between two superconductors to obtain a ϕ_0 -junction [37, 38].

In Ref. [41], we considered an equilibrium transverse spin current generated by a longitudinal charge supercurrent in a Josephson junction, which we will refer to here as the *superspin Hall current*. Whereas most studies of spin Hall effects in superconductors consider purely *s*-wave or quasiparticle effects [30–39], the superspin Hall current is the result of an interplay between the *s*-wave condensate of a conventional superconductor and a proximity-induced *p*-wave condensate. As opposed to the interfacial spin current considered in Ref. [40], the superspin Hall current considered in Ref. [41] arises in a magnetic Josephson junction. In Ref. [41] we also consider the ballistic limit, rather than the diffusive limit considered in Refs. [31, 37–39].

An open question regarding the superspin Hall current is whether or not it induces an edge spin magnetization which could serve as an experimental signature of its existence. This question was not addressed in Ref. [41], which considered periodic boundary conditions and thus in practice a cylindrical geometry.

In this paper, we present two main results. The first result is a full two-dimensional analysis of the superspin Hall *effect* where we are able to address the issue of what happens to the spin supercurrent at the edges of the system. This issue is of interest with respect to possible experimental probes of the effect.

* vetle.k.risinggard@ntnu.no

The second result is the prediction of a corresponding *inverse effect*, namely the inverse superspin Hall effect. In this case, an equilibrium spin current produces a transverse charge supercurrent, which gives rise to a ϕ_0 shift in the Josephson junction. The ϕ_0 shift is—as opposed to previous predictions of ϕ_0 junctions incorporating spin–orbit coupling and ferromagnets [19, 37, 38, 42]—induced by a pure equilibrium spin current. We propose that the ϕ_0 shift can be used to detect the spin-polarization of a supercurrent carried by Cooper pairs. Being an equilibrium property of the junction we consider, this detection scheme will not dissipate the equilibrium spin current. This offers a way to electrically and directly verify the spin polarization of previously detected long-ranged supercurrents [43–48].

The superspin Hall effect can not only be used to detect spin-polarized supercurrents, but also other equilibrium spin currents. To illustrate this we also calculate the ϕ_0 shift induced by the exchange spin current between two misaligned ferromagnets [49, 50].

II. INTRODUCTION TO THE SUPERSPIN HALL EFFECT

The intrinsic superspin Hall effect, which we considered in Ref. [41], arises in a magnetic Josephson junction with Rashba spin–orbit interlayers, see Fig. 1. When a phase difference ϕ is applied over the junction, so that a longitudinal charge current flows between the two superconductors, a transverse spin current is induced near the superconductor–Rashba-metal interface. Being transverse, it flows parallel to the interface (y direction). Its spin polarization is perpendicular to the exchange field \mathbf{h} in the ferromagnet—along the y direction for $\mathbf{h} = h\mathbf{e}_x$, and along the x direction for $\mathbf{h} = h\mathbf{e}_y$.

As we explain in Ref. [41], this spin supercurrent is the result of a delicate interplay between the different condensates in the junction. Consider for instance $\mathbf{h} = h\mathbf{e}_y$ and, for the sake of the argument, even-frequency superconducting correlations. In addition to the s -wave spin-singlet condensate emanating from the proximitized superconductors, there are also p -wave correlations in the junction due to the broken translation symmetry at the material interfaces [51, 52] and due to the presence of spin–orbit coupling [53]. Due to the overall antisymmetry of the Cooper-pair wave function, the spin state of these even-frequency p -wave correlations must be one (or several) of the triplet states. The generation of both short- and long-range triplets is possible because of the

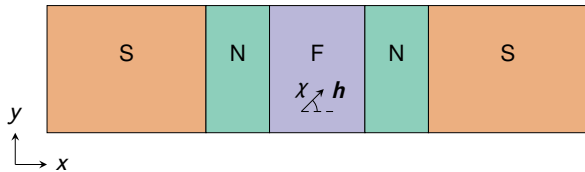


Figure 1. Suggested experimental setup for the superspin Hall effect. A magnetic Josephson junction in the clean limit with Rashba spin–orbit interlayers. The in-plane exchange field \mathbf{h} in the ferromagnet makes an angle χ with the x axis.

simultaneous presence of both ferromagnetism and spin–orbit coupling [13, 14]. As explained in Ref. [41], the interaction of the s - and p -wave condensates can be described via two different superconducting order parameters in the junction which quantify the superconducting correlations present in the system. These are, respectively, the sum Δ_+ and the difference Δ_- of the original s -wave and p -wave order parameters, Δ_s and Δ_k , where k refers to the momentum in the y direction. The momentum index k is a good quantum number for a system with periodic boundary conditions in the y direction, as the one considered in Ref. [41]. The relative magnitude of these order parameters is determined by the relative phase of the original s -wave and p -wave order parameters,

$$|\Delta_{\pm}|^2 = |\Delta_s|^2 + |\Delta_k|^2 \pm 2 \operatorname{Re}(\Delta_s \Delta_k^*). \quad (1)$$

When no phase difference is applied over the junction, the s -wave order parameter is purely real, whereas the p -wave order parameter is purely imaginary. Consequently, their sum and difference have equal magnitude, $|\Delta_+| = |\Delta_-|$, and as many Cooper pairs condense in the $|k \uparrow, -k \downarrow\rangle$ state as in the $|k \downarrow, -k \uparrow\rangle$ state. But, when a phase difference is applied, the s -wave order parameter acquires an imaginary component and the p -wave order parameter acquires a real component. In turn, their sum and difference are no longer equal, $|\Delta_+| \neq |\Delta_-|$, and Cooper pairs condense preferentially at either $|k \uparrow, -k \downarrow\rangle$ or $|k \downarrow, -k \uparrow\rangle$ because of the difference in condensation energies. Such a selective condensation gives rise to a nonzero k -resolved spin magnetization \mathbf{S}_k that is antisymmetric in k . Subsequently, this antisymmetric momentum-resolved spin magnetization produces a spin current polarized along the spin magnetization direction. For an exchange field $\mathbf{h} = h\mathbf{e}_y$ the momentum-resolved spin magnetization points in the x direction; thus the application of a longitudinal phase difference (charge current) has given rise to a transverse spin current polarized along \mathbf{e}_x .

III. THEORY

We consider a superconducting heterostructure in two dimensions in the clean limit, incorporating strong spin–orbit coupling. For this we use the tight-binding Bogoliubov–de Gennes framework [3]. Our heterostructure consists of superconductors, normal metals with Rashba spin–orbit coupling, and ferromagnets. Our Hamiltonian is

$$\begin{aligned} H = & -t \sum_{\langle i,j \rangle, \sigma} c_{i,\sigma}^\dagger c_{j,\sigma} - \sum_{i,\sigma} \mu_i c_{i,\sigma}^\dagger c_{i,\sigma} - \sum_i U_i n_{i,\uparrow} n_{i,\downarrow} \\ & - (i/2) \sum_{\langle i,j \rangle, \alpha, \beta} \lambda_i [\mathbf{n} \cdot (\boldsymbol{\sigma} \times \mathbf{d}_{ij})]_{\alpha\beta} c_{i,\alpha}^\dagger c_{j,\beta} \\ & + \sum_{i,\alpha,\beta} (\mathbf{h}_i \cdot \boldsymbol{\sigma})_{\alpha\beta} c_{i,\alpha}^\dagger c_{i,\beta}, \end{aligned} \quad (2)$$

where i and j are position indices ($i, j = 1, \dots, N_x N_y$, where N_x and N_y are the dimensions of the lattice); $\langle i, j \rangle$ indicates that i and j are nearest neighbors; t is the hopping integral; $c_{i,\sigma}^\dagger$ and $c_{i,\sigma}$ are electron creation and annihilation operators at site i for spin σ ; μ_i is the local chemical potential; U_i is

the local on-site attraction that gives rise to superconductivity ($U_i = 0$ outside the superconductors and $U_i = U > 0$ inside the superconductors); $n_{i,\sigma} = c_{i,\sigma}^\dagger c_{i,\sigma}$ is the number operator at site i for spin σ ; λ_i is the local Rashba parameter ($\lambda_i = 0$ outside the normal metals and $\lambda_i = \pm\lambda$ inside the normal metals); \mathbf{n} is the unit vector normal to the Rashba-metal/ferromagnet interface; $\boldsymbol{\sigma}$ is the vector of Pauli matrices; $\mathbf{d}_{ij} = -\mathbf{d}_{ji}$ is the vector pointing from site i to site j ; and \mathbf{h}_i is the local magnetic exchange field ($\mathbf{h}_i = 0$ outside the ferromagnet and $\mathbf{h}_i = \mathbf{h}$ inside the ferromagnet).

The two-particle Hubbard- U term can be recast as

$$-\sum_i U_i n_{i,\uparrow} n_{i,\downarrow} = \sum_i (\Delta_i c_{i,\downarrow}^\dagger c_{i,\downarrow}^\dagger + \Delta_i^\dagger c_{i,\downarrow} c_{i,\uparrow} + |\Delta_i|^2 / U_i) \quad (3)$$

using the standard mean-field *ansatz* $\Delta_i = -U_i \langle c_{i,\downarrow} c_{i,\uparrow} \rangle$. We symmetrize the Hamiltonian using the fundamental fermionic anticommutator to write

$$\sum_{\lambda,\kappa} A_{\lambda,\kappa} c_\lambda^\dagger c_\kappa = \frac{1}{2} \sum_\lambda A_{\lambda,\lambda} + \frac{1}{2} \sum_{\lambda,\kappa} A_{\lambda,\kappa} (c_\lambda^\dagger c_\kappa - c_\kappa c_\lambda^\dagger). \quad (4)$$

Introducing the basis

$$B_i^\dagger = \begin{pmatrix} c_{i,\uparrow}^\dagger & c_{i,\downarrow}^\dagger & c_{i,\uparrow} & c_{i,\downarrow} \end{pmatrix}, \quad (5)$$

we may then write the Hamiltonian on the form

$$H = H_0 + \frac{1}{2} \sum_{i,j} B_i^\dagger H_{ij} B_j. \quad (6)$$

Here, we have identified the constant term H_0 ,

$$H_0 = \sum_i |\Delta_i|^2 / U_i - \sum_i \mu_i, \quad (7)$$

where the first sum runs only over the superconductors, and the 4×4 matrix H_{ij} ,

$$\begin{aligned} H_{ij} = & \frac{1}{2} t \tau_z \sigma_0 \delta_{j,i+\delta} - \mu_i \tau_z \sigma_0 \delta_{i,j} + \frac{i}{2} \Delta_i \tau_+ \sigma_y \delta_{i,j} \\ & - \frac{i}{2} \Delta_i^\dagger \tau_- \sigma_y \delta_{i,j} - \frac{i}{4} \lambda_i \tau_0 \sigma_z (\delta_{j,i+\delta_y} - \delta_{j,i-\delta_y}) \\ & + h_i^x \tau_z \sigma_x \delta_{i,j} + h_i^y \tau_0 \sigma_y \delta_{i,j} + h_i^z \tau_z \sigma_z \delta_{i,j}, \end{aligned} \quad (8)$$

where $\delta_{i,j}$ is the Kronecker delta, we used $\mathbf{n} = \mathbf{e}_x$, we introduced the set of nearest neighbor vectors $\boldsymbol{\delta} = (\delta_x, \delta_y)$, and τ_n and σ_n are the Pauli matrices for $n = x, y, z$ and $n = 0$ refers to the identity. Moreover, $\tau_\pm = \tau_x \pm i\tau_y$, and products of Pauli matrices are interpreted as Kronecker products. As is the usual definition, $\tau_z \sigma_0$, for instance, evaluates to $\tau_z \sigma_0 = \text{diag}(+1, +1, -1, -1)$ [54].

The index structure in Eq. (6) is that of a matrix product, in which the matrix M is multiplied from the left with the row vector B^\dagger , and the resulting row vector is multiplied with the column vector B . Each element in M is a 4×4 matrix H_{ij} , and each element in B (or B^\dagger) is a 4×1 (or 1×4) column (or row).

The structure of the matrix M is determined by how we combine the elements of B and B^\dagger into vectors. We consider a square lattice. The position indices i and j run over the entire system ($N_x \times N_y$ sites). Since each pair (i, j) corresponds to a 4×4 block H_{ij} , we expect M to be a $4N_x N_y \times 4N_x N_y$ matrix.

By choosing some enumeration scheme for the sites i (such as the one in Fig. 2), we can thus write

$$H = H_0 + \frac{1}{2} B^\dagger M B, \quad (9)$$

and diagonalize M by the techniques that are familiar from linear algebra. Since H is Hermitian, so is M , and M can thus be diagonalized as $M = P E P^{-1}$, where E is diagonal and real, and P is unitary, $P^{-1} = P^\dagger$ [55]. Substituting $M = P E P^{-1}$ into Eq. (9) we obtain

$$H = H_0 + \frac{1}{2} \sum_n E_n \gamma_n^\dagger \gamma_n, \quad (10)$$

where we defined the new quasiparticle operators $\gamma^\dagger = B^\dagger P$ and $\gamma = P^{-1} B$, γ_n is the n th element of γ , E_n is the n th eigenenergy, and $n = 1, \dots, 4N_x N_y$. The original electron operators can be related to the quasiparticle operators by

$$\begin{aligned} c_{i,\uparrow} &= \sum_n u_{i,n} \gamma_n, & c_{i,\downarrow} &= \sum_n v_{i,n} \gamma_n, \\ c_{i,\uparrow}^\dagger &= \sum_n w_{i,n} \gamma_n, & c_{i,\downarrow}^\dagger &= \sum_n x_{i,n} \gamma_n, \end{aligned} \quad (11)$$

where $u_{i,n}$ with $i = 1, \dots, N_x N_y$ is, respectively, P_{ln} with $l = 1, 5, 9, \dots$. Likewise, $v_{i,n}$ with $i = 1, \dots, N_x N_y$ is P_{ln} with $l = 2, 6, 10, \dots$; $w_{i,n}$ with $i = 1, \dots, N_x N_y$ is P_{ln} with $l = 3, 7, 11, \dots$; and $x_{i,n}$ with $i = 1, \dots, N_x N_y$ is P_{ln} with $l = 4, 8, 12, \dots$.

We can now derive expressions for any of the observables in the system in terms of the eigenenergies E_n and the eigenvectors $u_{i,n}$, $v_{i,n}$, $w_{i,n}$, and $x_{i,n}$. For instance, the superconducting gap takes the form

$$\Delta_i = U_i \sum_n v_{i,n} w_{i,n}^* f(E_n/2), \quad (12)$$

and the spin magnetization takes the form

$$\langle S_i^x \rangle = 2 \sum_n \text{Re}(u_{i,n}^* v_{i,n}) f(E_n/2), \quad (13a)$$

$$\langle S_i^y \rangle = 2 \sum_n \text{Im}(i u_{i,n}^* v_{i,n}) f(E_n/2), \quad (13b)$$

$$\langle S_i^z \rangle = \sum_n (|u_{i,n}|^2 - |v_{i,n}|^2) f(E_n/2). \quad (13c)$$

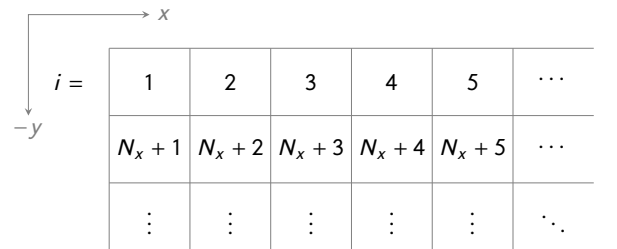


Figure 2. Enumeration scheme for the $N_x \times N_y$ square lattice. The site index i is incremented site by site along the rows, starting in the upper left corner.

The free energy reads

$$F = H_0 - \frac{1}{\beta} \sum_n \ln[1 + \exp(-\beta E_n/2)], \quad (14)$$

where $1/\beta = T$, and T is temperature.

Expressions for the charge and spin currents can be obtained from their respective continuity equations,

$$\partial_t \rho_i = -\nabla \cdot \mathbf{j}_i, \quad (15)$$

and

$$\partial_t \mathbf{s}_i = -\nabla \cdot \mathbf{J}_i, \quad (16)$$

where ρ_i is the charge density at i , \mathbf{j}_i is the current density at i , \mathbf{s}_i is the spin density at i , \mathbf{J}_i is the spin-current-density tensor at i , and the gradient of the spin-current-density tensor is taken with respect to the position variables. Note that the spin current defined by the spin continuity equation is only conserved in regions without ferromagnetism or spin-orbit coupling because these terms are spin nonconserving [56]. For each of the two continuity equations, we find expressions for the currents by integrating the equations over space to obtain (for the case of the charge current)

$$\partial_t Q_i = - \int_{\Omega} d\mathbf{r} (\nabla \cdot \mathbf{j}_i),$$

where $Q_i = \sum_{\sigma} c_{i,\sigma}^{\dagger} c_{i,\sigma}$ is the charge at i and Ω is the unit-cell volume. The integral on the right-hand side can be evaluated using Green's theorem,

$$\int_{\Omega} d\mathbf{r} (\nabla \cdot \mathbf{j}_i) = \int_{\partial\Omega} dS (\mathbf{j}_i \cdot \mathbf{e}_n) = \sum_l j_{i,l} a = \sum_l I_{i,l},$$

where $\partial\Omega$ is the unit-cell boundary, \mathbf{e}_n is the outward-pointing boundary normal, and a is the unit-cell side length. Since we consider a square lattice, $I_{i,l}$ is the current through the l th face of the square unit cell. The left-hand side of the continuity equation can be evaluated using Heisenberg's equation of motion. Thus the sum of currents out of the unit cell is

$$\sum_l I_{i,l} = -i[H, Q_i]. \quad (17)$$

Evaluating the commutator and taking a combined thermal and quantum-mechanical average gives the charge current in the x direction

$$\langle I_i^x \rangle = t \sum_n \text{Im}(u_{i+1,n}^* u_{i,n} - u_{i-1,n}^* u_{i,n} + v_{i+1,n}^* v_{i,n} - v_{i-1,n}^* v_{i,n}) f(E_n/2) \quad (18)$$

and in the y direction

$$\begin{aligned} \langle I_i^y \rangle = t \sum_n \text{Im}(u_{i-N_x,n}^* u_{i,n} - u_{i+N_x,n}^* u_{i,n} \\ + v_{i-N_x,n}^* v_{i,n} - v_{i+N_x,n}^* v_{i,n}) f(E_n/2) \\ - \frac{1}{2} \sum_n \lambda_i \text{Re}(u_{i-N_x,n}^* u_{i,n} + u_{i+N_x,n}^* u_{i,n} \\ - v_{i-N_x,n}^* v_{i,n} - v_{i+N_x,n}^* v_{i,n}) f(E_n/2). \end{aligned} \quad (19)$$

A similar procedure for the spin currents gives the three spin components of the spin current in the x direction

$$\langle I_i^{xx} \rangle = t \sum_n \text{Im}(u_{i+1,n}^* v_{i,n} + v_{i+1,n}^* u_{i,n} - u_{i-1,n}^* v_{i,n} - v_{i-1,n}^* u_{i,n}) f(E_n/2), \quad (20)$$

$$\langle I_i^{xy} \rangle = t \sum_n \text{Re}(u_{i+1,n}^* v_{i,n} - v_{i+1,n}^* u_{i,n} - u_{i-1,n}^* v_{i,n} + v_{i-1,n}^* u_{i,n}) f(E_n/2), \quad (21)$$

$$\langle I_i^{xz} \rangle = t \sum_n \text{Im}(u_{i+1,n}^* u_{i,n} - v_{i+1,n}^* v_{i,n} - u_{i-1,n}^* u_{i,n} + v_{i-1,n}^* v_{i,n}) f(E_n/2), \quad (22)$$

and likewise the three spin components of the spin current in the y direction

$$\langle I_i^{yx} \rangle = t \sum_n \text{Im}(u_{i-N_x,n}^* v_{i,n} + v_{i-N_x,n}^* u_{i,n} - u_{i+N_x,n}^* v_{i,n} - v_{i+N_x,n}^* u_{i,n}) f(E_n/2), \quad (23)$$

$$\langle I_i^{yy} \rangle = t \sum_n \text{Re}(u_{i-N_x,n}^* v_{i,n} - v_{i-N_x,n}^* u_{i,n} - u_{i+N_x,n}^* v_{i,n} + v_{i+N_x,n}^* u_{i,n}) f(E_n/2), \quad (24)$$

$$\langle I_i^{yz} \rangle = t \sum_n \text{Im}(u_{i-N_x,n}^* u_{i,n} - v_{i-N_x,n}^* v_{i,n} - u_{i+N_x,n}^* u_{i,n} + v_{i+N_x,n}^* v_{i,n}) f(E_n/2). \quad (25)$$

A general superconducting order parameter F can be decomposed into a spin-singlet and a spin-triplet contribution [57],

$$F = (\psi + \mathbf{d} \cdot \boldsymbol{\sigma}) i\sigma_y, \quad (26)$$

where ψ is the singlet amplitude and the \mathbf{d} vector is the vector of triplet amplitudes along the x , y , and z axes,

$$\mathbf{d} = \frac{1}{2}[\Delta_{\downarrow\downarrow} - \Delta_{\uparrow\uparrow}, -i(\Delta_{\downarrow\downarrow} + \Delta_{\uparrow\uparrow}), 2\Delta_{\uparrow\downarrow}]. \quad (27)$$

The spin structure of the singlet amplitude is already familiar from Eq. (8), where the same factor $i\sigma_y$ appears. In a unitary superconducting state, the identity $F^\dagger = F^{-1}$ holds, and FF^\dagger is proportional to the identity. A general superconducting system is, however, not unitary, and straightforward calculation shows that

$$FF^\dagger = |\psi|^2 + |\mathbf{d}|^2 + \boldsymbol{\sigma} \cdot [(\psi \mathbf{d}^* + \psi^* \mathbf{d}) + i(\mathbf{d} \times \mathbf{d}^*)]. \quad (28)$$

The term $i(\mathbf{d} \times \mathbf{d}^*)$ is proportional to the spin expectation value of the pure triplet Cooper pairs [57], whereas the term $(\psi \mathbf{d}^* + \psi^* \mathbf{d})$ is proportional to the spin magnetization arising due to coexistence of singlet and triplet pairing [41],

$$S_{\text{Cooper}} \propto (\psi \mathbf{d}^* + \psi^* \mathbf{d}) + i(\mathbf{d} \times \mathbf{d}^*). \quad (29)$$

In order to calculate the Cooper-pair spin magnetization, we need expressions for the superconducting amplitudes. The s -wave singlet amplitude $S_{i,0}$ at i is identical to the gap we calculated in Eq. (12), except for the factor U_i ,

$$S_0 = \frac{1}{2}[\langle c_{i,\uparrow} c_{i,\downarrow} \rangle - \langle c_{i,\downarrow} c_{i,\uparrow} \rangle] = \sum_n v_{i,n} w_{i,n}^* f(E_n/2). \quad (30)$$

The direct and inverse superspin Hall effects depend on the existence of even-frequency, p_y -wave, spin-triplet amplitudes,

$$\begin{aligned}\mathcal{P}_{i,\uparrow\downarrow}^y &= \frac{1}{2} \sum_{\pm} \pm [\langle c_{i,\uparrow} c_{i\pm\delta_y, \downarrow} \rangle + \langle c_{i,\downarrow} c_{i\pm\delta_y, \uparrow} \rangle] \\ &= \frac{1}{2} \sum_{n,\pm} \pm (w_{i,n}^* v_{i\mp N_x, n} - v_{i,n} w_{i\mp N_x, n}^*) f(E_n/2),\end{aligned}\quad (31a)$$

$$\begin{aligned}\mathcal{P}_{i,\uparrow\uparrow}^y &= \sum_{\pm} \pm \langle c_{i,\uparrow} c_{i\pm\delta_y, \uparrow} \rangle \\ &= \sum_{n,\pm} \pm w_{i,n}^* u_{i\mp N_x, n} f(E_n/2),\end{aligned}\quad (31b)$$

$$\begin{aligned}\mathcal{P}_{i,\downarrow\downarrow}^y &= \sum_{\pm} \pm \langle c_{i,\downarrow} c_{i\pm\delta_y, \downarrow} \rangle \\ &= \sum_{n,\pm} \pm x_{i,n}^* v_{i\mp N_x, n} f(E_n/2).\end{aligned}\quad (31c)$$

In Sect. V we will need the odd-frequency, s -wave, spin-triplet amplitudes,

$$\begin{aligned}\mathcal{S}_{i,\uparrow\downarrow}(t) &= \frac{1}{2} [\langle c_{i,\uparrow}(t) c_{i,\downarrow}(0) \rangle + \langle c_{i,\downarrow}(t) c_{i,\uparrow}(0) \rangle] \\ &= \frac{1}{2} \sum_n (w_{i,n}^* v_{i,n} - x_{i,n}^* u_{i,n}) f(E_n/2) e^{iE_n t/2},\end{aligned}\quad (32a)$$

$$\begin{aligned}\mathcal{S}_{i,\uparrow\uparrow}(t) &= \langle c_{i,\uparrow}(t) c_{i,\uparrow}(0) \rangle \\ &= \sum_n w_{i,n}^* u_{i,n} f(E_n/2) e^{iE_n t/2},\end{aligned}\quad (32b)$$

$$\begin{aligned}\mathcal{S}_{i,\downarrow\downarrow}(t) &= \langle c_{i,\downarrow}(t) c_{i,\downarrow}(0) \rangle \\ &= \sum_n x_{i,n}^* v_{i,n} f(E_n/2) e^{iE_n t/2}.\end{aligned}\quad (32c)$$

IV. NUMERICAL CALCULATIONS

In this article, we consider the three setups in Figs. 1, 7, and 9. In each case, we construct the matrix M from Eq. (9) and diagonalize it to find the eigenvalues and eigenvectors. Using these, we may calculate physical quantities such as the superconducting gap Δ_i or the spin magnetization $\langle S_i \rangle$. Because the matrix M depends on the superconducting gap, the equations must be solved self-consistently by substituting the gap calculated using Eq. (12) back into M and iterating.

For each of the systems we consider, we make sure that the superconducting state minimizes the free energy in Eq. (14). In all the systems, we take the exchange field \mathbf{h}_i of the ferromagnets to be an external parameter, that is, we do not calculate the exchange field self-consistently. This is consistent with an s - d -type model in which the localized d electrons are responsible for the magnetic behavior [58, 59]. The spin magnetization $\langle S_i \rangle$ that we calculate is thus the spin polarization of the itinerant s electrons.

In the setup in Fig. 1 we consider the injection of a charge current into the junction by an applied phase difference. This is accomplished by fixing the phase of the superconducting gap Δ_i at the leftmost lattice points in the left superconductor and at the rightmost lattice points in the right superconductor. The applied phase difference between these points can be used as a

proxy for the applied phase difference over the junction (N/F/N spacer) because the phase drop inside the superconductors is typically small. (Fixing the phase difference at $\Delta\phi = 0.5\pi$ gives an effective phase difference over the N/F/N spacer of $\Delta\phi \approx 0.47$ – 0.48π .)

In the setup in Fig. 7 we consider the injection of a charge current across the injection junction by an applied phase difference. We fix the phase of the left superconductor in the detector at $\phi = 0$ (this choice is arbitrary—only phase differences matter). By varying the phase of the right superconductor from 0 to 2π we calculate the current–phase and free-energy–phase relation of the detector junction. We take the induced anomalous phase ϕ_0 to be the phase over the detector that minimizes the free energy and gives $\langle I^x \rangle = I(-\phi_0) = 0$.

In the setup in Fig. 9 we consider the injection of an exchange spin current from two misaligned ferromagnets. We fix the phase of both superconductors at $\phi = 0$ and calculate the anomalous charge current $I(0) = \langle I^x \rangle$. In its simplest form, a ϕ_0 junction [60–63] has the current–phase relation $I(\phi) = I_c \sin(\phi + \phi_0)$. For small ϕ_0 shifts, the anomalous phase ϕ_0 and the anomalous current $I(0) = I_c \sin \phi_0$ are proportional, $I(0) \approx I_c \phi_0$. Therefore, we can use the anomalous current as a proxy for the anomalous phase.

The advantage of tight-binding Bogoliubov–de Gennes framework [3] that we use is that it is not subject to the limitations on length and energy scales that are inherent to for instance quasi-classical theory [64]. However, using this tight-binding framework, only comparatively small lattice sizes are computationally manageable, especially in two-dimensional finite-size calculations. For superconducting structures, the relevant length scale is the superconducting coherence length $\xi = \hbar v_F / \pi \Delta$ [2, 3]. If the coherence length is to be smaller than the thickness of the superconducting layers, this requires relatively large values of the superconducting gap and large critical temperatures. Nonetheless, the tight-binding framework can still be used to make qualitative and quantitative predictions for experimentally relevant systems. To do this requires that the spatial dimensions are scaled by the superconductive coherence length. One example of a successful application of this method is Ref. [65], whose predictions correspond very well to the experimental results of Ref. [66].

We take a similar approach. With the parameters chosen in Sect. V–VIII the thickness of the superconducting layers is about one coherence length, and the normal-metal and ferromagnetic layers vary from about $\xi/4$ to 2ξ . As long as the weak links are not orders of magnitude larger than the coherence length, the qualitative features of our results are robust towards variations of the system size. In particular, the ϕ_0 shift that we calculate in Sect. VII is nearly independent of the length of the detector junction.

V. SUPERSPIN HALL EFFECT IN TWO DIMENSIONS: SPIN CURRENT AND EDGE MAGNETIZATION

Our analysis of the superspin Hall effect in Ref. [41] was an effective one-dimensional analysis in the sense that we assumed periodic boundary conditions in the y direction and thus could

get rid of the y coordinate by Fourier transformation. Whereas we were still able to calculate the transverse spin current, this left open the question of the exact spin current circulation pattern and whether any spin magnetization arises at the edges of the sample. The latter would be a useful experimental signature of the superspin Hall effect, as it has been previously for the (nonequilibrium) spin Hall effect [67, 68].

In the usual nonsuperconducting, nonequilibrium spin Hall effect, spin accumulates at the edges of the sample because the transverse spin current has nowhere to go upon reaching the sample boundary [21]. A steady state is achieved because the spin Hall effect is found in materials with strong spin-orbit coupling where spin is not conserved. The accumulated spin at the edge at any time is thus the result of a balance between influx of spin from the bulk and spin loss due to spin-orbit coupling.

We find that the superspin Hall current does not give rise to a spin magnetization at the sample edges by this familiar mechanism. The simple reason is that the superspin Hall current in our system does have somewhere to go—it can be drained from the superconductor, where in our model spin is conserved, into the Rashba-metal/ferromagnet spacer, where spin is not conserved. This circulation of the superspin Hall current from the spacer, into the superconductor, and back into the spacer, is shown in Fig. 3(a).

Note that, although the net flow of spin is from the bottom of the sample to the top, the direction of the spin current (up/down) oscillates as a function of the distance into the superconductor [Fig. 3(b)]. As explained in Ref. [41], the oscillation period is a function of the system parameters, such as the strength of the spin-orbit coupling in the normal layer and the strength of the exchange field in the ferromagnet. The period varies from atomic-scale oscillations to roughly a fourth of the coherence length. Such rapid oscillations are characteristic for physical quantities in ballistic quantum-mechanical systems. For instance, they can also be found in the proximity-induced magnetization in conventional superconductors [69] and helical edge-mode currents in triplet superconductors [70].

Although the superspin Hall current does not give rise to a spin magnetization at the edges of the sample, there *is* an x -polarized spin magnetization at the edges of the system [Fig. 4(a)]. However, contrary to what we would expect from a spin magnetization arising due to accumulation of spins deposited by the superspin Hall current, the spin magnetization sign pattern that we observe is $\pm\mp$, not $\pm\pm$, where the signs refer to the left upper/lower and right upper/lower edges, respectively. Furthermore, its amplitude varies as $\cos \phi$, where ϕ is the phase difference applied between the two superconductors [Fig. 5(a)]. We would expect a spin magnetization induced by the superspin Hall current—which is again induced by the longitudinal charge current—to have an amplitude that varied as $\sin \phi$ [compare with Fig. 5(c) and (d)].

The momentum-resolved spin magnetization that gives rise to the superspin Hall current is the result of the interaction of the s -wave spin-singlet and a p -wave spin-triplet condensate, both even in frequency. The edge spin magnetization we observe in Fig. 4, on the other hand, is the result of the interaction of the even-frequency, s -wave, spin singlet condensate and an

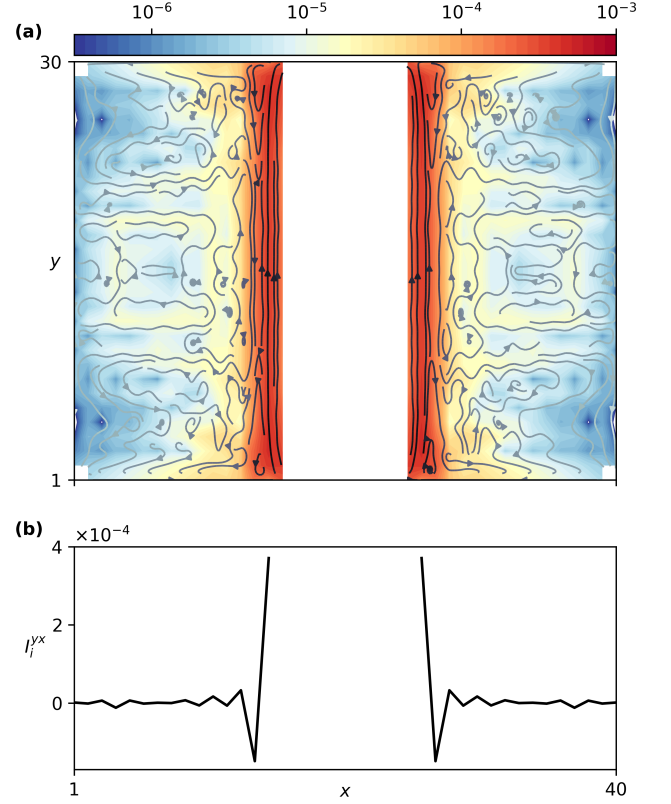


Figure 3. Superspin Hall current in two dimensions at phase difference $\phi = \pi/2$. (a) Circulation pattern of the x component of the spin current. The spin current is only plotted in the superconductors, where spin is conserved. (b) Cut along the x direction at $y = 15$ inside the superconductors. The spin current oscillates as a function of the distance from the N/F/N weak link into the superconductors. We use the following parameter values: the system size is $N_x = 40$ times $N_y = 30$; the layer thicknesses are $N_S = 15$, $N_N = 3$, and $N_F = 4$; the chemical potentials are $\mu_S = 0.9$, $\mu_N = 0.85$, and $\mu_F = 0.8$; the Rashba spin-orbit coupling in the normal metal is $\lambda = 0.3$, the exchange field in the ferromagnet is $h_y = 0.15$ ($h_x = h_z = 0$), the on-site attraction in the superconductor is $U = 1.1$, and the temperature is $T = 0.01$. All energies are normalized with respect to the hopping parameter ($t = 1$).

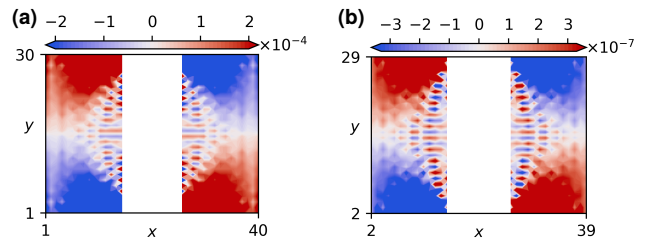


Figure 4. x component of the spin magnetization at phase difference $\phi = 0$. (a) The total spin magnetization. (b) The spin magnetization induced by interaction of s -wave singlets and odd-frequency, s -wave triplets (arbitrary units). Except for the applied phase between the superconductors, all parameters are identical to Fig. 3.

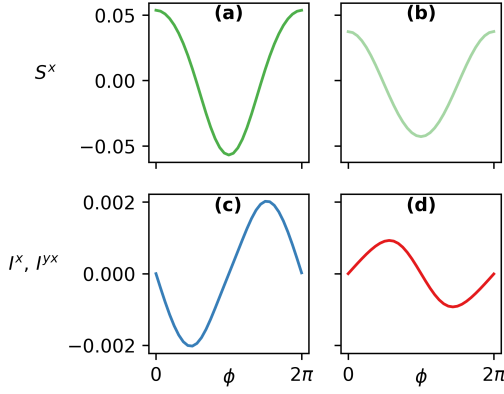


Figure 5. Phase dependence of the superspin Hall effect. (a) Total spin magnetization $\langle S^x \rangle$ summed over the lower half of the right superconductor. (b) Cooper-pair spin magnetization S_{Cooper}^x summed over the lower half of the right superconductor (arbitrary units). (c) Longitudinal charge current $\langle I^x \rangle$ summed over the y cross section. (d) Transverse spin current $\langle I^{yx} \rangle$ summed over the x cross section. All parameters are identical to Fig. 3.

odd-frequency, s -wave, spin-triplet condensate. In Fig. 4(a) we have plotted the x component of the total spin magnetization calculated using Eq. (13a). In Fig. 4(b) we have plotted the x component of the spin magnetization calculated using Eq. (29), where we have used the superconducting amplitudes in Eq. (30) and Eq. (32). Apart from a constant prefactor, the plots are essentially identical. The spin magnetization due to the odd-frequency, s -wave spin triplets also reproduce the phase dependence of the total spin magnetization [compare Fig. 5(a) and (b)].

The fact that the edge spin magnetization is due to the odd-frequency triplets (s wave) whereas the superspin Hall effect is due to the even-frequency triplets (p wave) makes it clear that the spin magnetization is not a consequence of the superspin Hall current. Further evidence to this effect is that this particular spin magnetization is also predicted in the diffusive limit [71], where the superspin Hall effect is precluded because of the absence of p -wave correlations. Consequently, one can exist independently of the other—they are independent effects.

Nonetheless, the symmetries of the spin magnetization with respect to sign change of the Rashba spin-orbit coupling and the direction of the exchange field is the same as those of the superspin Hall current. In particular, rotating the exchange field by 90° from $\mathbf{h} = h\mathbf{e}_y$ to $\mathbf{h} = h\mathbf{e}_x$ also rotates the spin-triplet spin magnetization by 90° from x to y .

The temperature $T = 0.01$ (in units of t), which we chose for the simulations above, is well below the superconducting transition temperature, $T = 0.01 \lesssim T_c/2$. However, at still lower temperatures, Andreev bound states [72, 73] with a more dispersive energy-phase relation appear in the junction. The appearance of such states is common in ballistic systems with high interface transparencies and low temperatures. Because these states bounce multiple times between the two superconductors, they produce higher-harmonic contributions to the

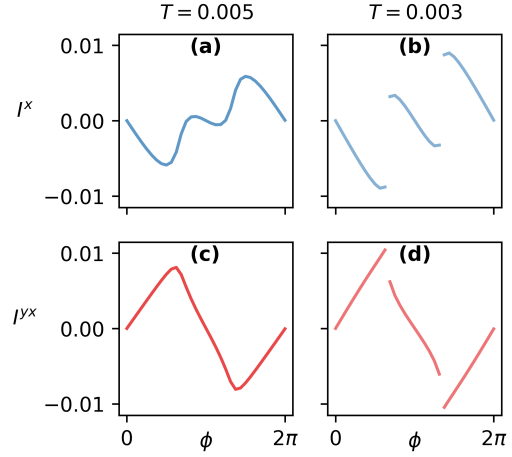


Figure 6. Phase dependence of the superspin Hall effect at low temperatures. (a) Longitudinal charge current $\langle I^x \rangle$ at $T = 0.005$ summed over the y cross section. (b) Longitudinal charge current $\langle I^x \rangle$ at $T = 0.003$ summed over the y cross section. (c) Transverse spin current $\langle I^{yx} \rangle$ at $T = 0.005$ summed over the x cross section. (d) Transverse spin current $\langle I^{yx} \rangle$ at $T = 0.003$ summed over the x cross section. All parameters except the temperature are identical to Fig. 3.

current-phase relation. The higher harmonics will distort the pure sinusoidal shape of the current-phase relation and may even introduce discontinuities [74, 75]. This, of course, also affects the superspin Hall current, as shown in Fig. 6.

The presence of Andreev bound states in the junction also affects the spin magnetization, which deviates from a pure cosine as a function of the applied phase difference ϕ . Interestingly, there is also a discernible difference between the total spin magnetization and the Cooper-pair spin magnetization computed via Eq. (29) at low temperatures.

VI. INVERSE SUPERSPIN HALL EFFECT

The Onsager reciprocal of the usual nonsuperconducting, nonequilibrium spin Hall effect is the inverse spin Hall effect—that is, injection of a transverse spin current generates a longitudinal charge current. In steady-state, the charge current must either be drained into external leads, or a voltage accumulates which exactly cancels the inverse spin Hall current. Analogously, one might expect that there should exist an inverse of the superspin Hall effect discussed in Sect. V—injecting an equilibrium transverse spin current should give rise to a longitudinal charge supercurrent [76]. However, in the absence of external leads, the steady state will be one with zero charge current. Instead, a phase difference ϕ_0 accumulates over the junction. This phase difference gives rise to a supercurrent that exactly cancels the one induced by the inverse superspin Hall effect. In this work, we confirm this expectation and find that the experimental signature of the inverse superspin Hall effect is a ϕ_0 junction.

VII. ELECTRICAL DETECTION OF THE SUPERCURRENT SPIN POLARIZATION

We propose to use the setup in Fig. 7 to detect the spin polarization of a supercurrent. This four-terminal setup consists of two perpendicular Josephson junctions. The charge supercurrent in the y direction injected into the S/F(y)/F(x)/F(y)/S junction is spin polarized in the x direction by the magnetic inhomogeneity provided by the F(y) layers. The transverse spin current thus injected into the S/N/F(x)/N/S junction induces a phase difference ϕ_0 between the left and right superconductors.

By applying a phase bias over the injection junction, a spin-polarized supercurrent is produced by the combined processes of spin mixing in the S/F(y) bilayer and spin rotation (rotation of spin quantization axis between the F(y) and F(x) layers). The current is spin-polarized in the x direction. The proximity to the F(y) layers provides the necessary conditions for the superspin Hall mechanism. Thus, the inverse superspin Hall effect converts this transverse spin current into a longitudinal charge supercurrent in the detector that flows from the left to the right superconductor. Consequently, in the steady state the detection junction is a ϕ_0 junction. If the two terminals of the detection junction are connected to form a superconducting loop, the current–phase relation of the detector can be measured by threading a magnetic flux through the loop [77]. The anomalous current $I(0) = I_c \sin \phi_0$ can also be measured directly using a SQUID in zero applied flux.

Fig. 8(a) and (b) show the current–phase and the free-energy–phase relation of the detector junction. At an applied phase difference of $\phi = 0$ over the injector junction [Fig. 8(a)] no spin current is injected across the detector. Consequently, the current–phase relation of the detector junction is that of an ordinary 0 junction. At an applied phase difference of $\phi = \pi/2$ over the injector junction [Fig. 8(b)] a large spin current is injected across the detector. Consequently, the current–phase relation is shifted by an amount $\phi_0 = -0.2\pi$.

Fig. 8(c) shows the complete ϕ_0 –phase relation. The abscissa corresponds to the applied phase difference of the injection junction. On the right ordinate we have plotted the charge and spin currents injected across the detector, that is, $\langle I^y \rangle$ and $\langle I^{yx} \rangle$. The $\langle I^y \rangle$ –phase and the $\langle I^{yx} \rangle$ –phase relations are both almost sinusoidal, and we interpret the spin current as the spin polarization of the charge current. On the left ordinate we have plotted the induced ϕ_0 shift, *i.e.* the phase ϕ over the detector that corresponds to $\langle I^x \rangle = 0$ and $F = F_{\min}$. Clearly, the ϕ_0 shift

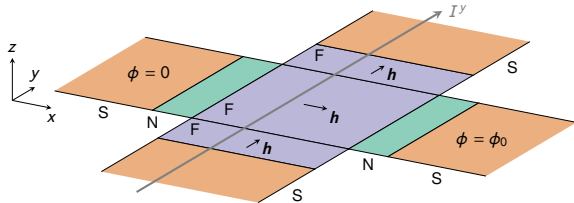


Figure 7. Proposed experimental setup for detecting a spin-polarized supercurrent consisting of two crossed Josephson junctions. The charge supercurrent in the y direction injected into the S/F(y)/F(x)/F(y)/S junction is spin polarized in the x direction by the magnetic inhomogeneity provided by the F(y) layers. The transverse spin current thus injected into the S/N/F(x)/N/S junction induces a phase difference ϕ_0 between the left and right superconductors.

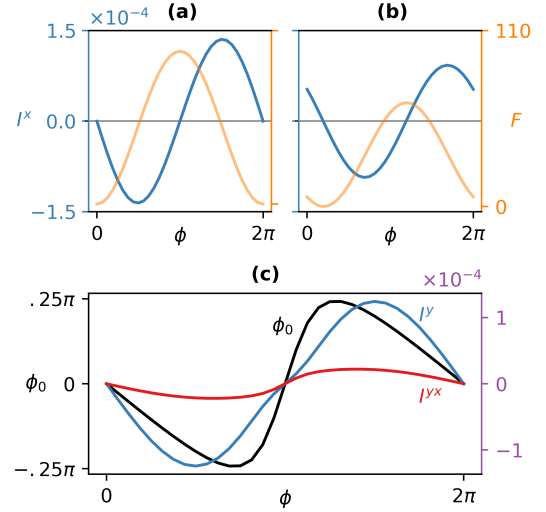


Figure 8. ϕ_0 effect for the setup in Fig. 7. (a) and (b): Current–phase relation and free-energy–phase relation of the detector junction as a function of the phase difference applied over the detector junction at applied phase differences of (a) $\phi = 0$ (no injected charge current) and (b) $\phi = \pi/2$ (maximal injected charge current) over the injection junction. In (b) a ϕ_0 shift of $\phi_0 = -0.2\pi$ is clearly visible. (c) Right ordinate: the injected charge current and the resulting spin current through the injection junction as a function of the phase difference applied over the injection junction. Left ordinate: the induced ϕ_0 shift in the detection junction as a function of the phase difference applied over the injection junction. The system size is $N_x = 35$ times $N_y = 21$. The layer thicknesses of the detector are $N_S = 5$, $N_N = 10$, and $N_F = 5$, and the layer thicknesses of the injector are $N_S = 5$, $N_{F(x)} = 3$, and $N_{F(y)} = 5$. All material parameters are identical to Fig. 3.

is zero when the transverse spin current is zero. Moreover, the sign of the ϕ_0 shift is a good predictor for the sign of the spin current. We have not been able to find a simple explanation for the deviation of the ϕ_0 shift from a pure sine, but the fact that both the sign and zeros of the anomalous phase ϕ_0 follow the spin supercurrent is consistent with the latter being the origin of the anomalous phase shift.

In addition to serving as a measurement of the spin polarization of the supercurrent, the setup we propose in Fig. 7 can also serve as a current-controlled phase battery. Such functionality has recently been proposed for a voltage-controlled ϕ_0 junction [78], and recent experiments have made progress towards both magnetic and electric phase control [62, 79].

VIII. ELECTRICAL DETECTION OF AN EXCHANGE SPIN CURRENT

The inverse superspin Hall effect is not only induced by a spin-polarized charge supercurrent, but also by other equilibrium spin currents. To demonstrate this, we consider the setup in Fig. 9. Here, the injection junction has been replaced by an F/N/F spin valve (no spin–orbit coupling in N). By misaligning the ferromagnets, we can inject an exchange spin current [49, 50]. The spin current is proportional to the sine of

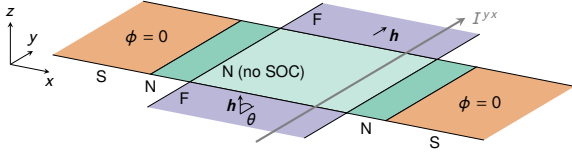


Figure 9. Suggested experimental setup for the inverse superspin Hall effect. The misalignment of the two ferromagnets (misalignment angle θ) produces a transverse exchange spin current that gives rise to an anomalous current between the two superconductors.

the misalignment angle θ , $I_s \sim \sin \theta$.

In Fig. 10(a) we plot the resulting spin current $\langle I^{yx} \rangle$ in the central normal metal (where spin is conserved) and the anomalous current $I(0) = \langle I^x \rangle$ as a function of the misalignment angle θ . The spin current is sinusoidal as a function of θ , consistent with the prediction of Ref. [49, 50]. The sinusoidal response of the anomalous current is consistent with our interpretation that it is induced by the exchange spin current (and not directly induced by the transverse variation in the exchange field as in Ref. [37]).

In Fig. 10(b) and (c) we plot the current–phase relation at a misalignment angle $\theta = 0$ and $\theta = \pi/2$. The anomalous current $I(0)$ shows up as a ϕ_0 shift of the current–phase relation.

In Fig. 11 we have plotted the magnitude and phase of the resulting superconducting gap. The oscillations in the gap magnitude $|\Delta_i|$ at the sample edges are due to Fridel oscillations

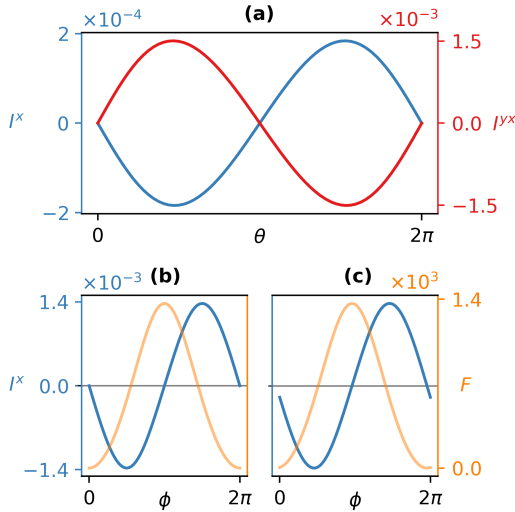


Figure 10. (a) Injected spin current $\langle I^{yx} \rangle$ in the central normal metal (no spin–orbit coupling) and anomalous current $I(0) = \langle I^x \rangle$ as a function of the misalignment angle θ . (b) and (c): Current–phase relation and free-energy–phase relation at a misalignment angle of respectively $\theta = 0$ (no injected spin current) and $\theta = \pi/2$ (maximal injected spin current). A ϕ_0 shift of $\phi_0 \approx -0.04\pi$ is clearly visible. We use the following parameter values: the system size is $N_x = 38$ times $N_y = 12$; the layer thicknesses of the detector are $N_S = 15$, $N_N = 2$, and $N_{N'} = 4$ and the layer thicknesses of the injector are $N_F = 1$ and $N_{F'} = 10$; the Rashba spin–orbit coupling is $\lambda = 1.87$; and the exchange field is $h = 0.8$. The remaining parameter values are identical to Fig. 3.

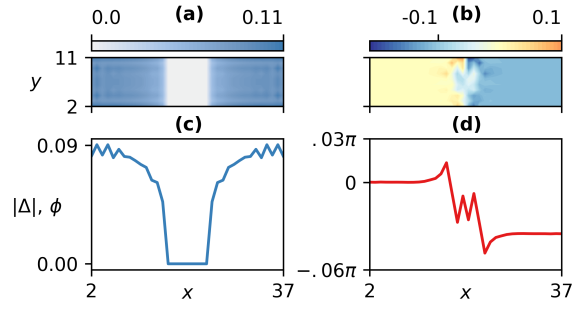


Figure 11. ϕ_0 signature of the inverse superspin Hall effect. (a) and (c): Magnitude of the superconducting gap $|\Delta_i|$. The gap vanishes in the N/F/N spacer and the inverse proximity effect is clearly visible. The oscillations of the gap at the edges of the sample are due to Fridel oscillations. (b) and (d): Phase of the s -wave singlet amplitude $S_{i,0}$. A ϕ_0 shift of $\phi_0 \approx -0.04\pi$ is clearly visible. The plots in panels (c) and (d) are for $y = 5$. We use parameter values that are identical to Fig. 10.

that create an oscillating charge density [80]. A ϕ_0 shift of $\phi_0 \approx -0.04\pi$ is clearly visible.

Fig. 12 shows the dependence of the anomalous current $I(0)$ on the spin–orbit coupling strength λ in the Rashba metals and the exchange-field strength h in the ferromagnets. There is a pronounced peak (or dip) at $h \approx 0.8$ and $\lambda \approx 1.9$. This parameter dependence can be understood as follows: We expect the inverse superspin Hall effect to disappear when the exchange field vanishes because $h = 0$ means that no transverse spin current is injected. (Also, magnetism is a prerequisite for the superspin Hall effect.) For small values of h , we expect the anomalous current to increase with the exchange field because an increase in h leads to an increase in the transverse spin current. However, for large values of h we expect the superspin Hall effect to disappear because the exchange field suppresses the superconducting proximity effect.

We also expect the anomalous current to vanish for vanishing spin–orbit coupling because spin–orbit coupling is a prerequisite for the superspin Hall effect. For finite λ there is a finite anomalous current because of the superspin Hall effect, but we expect the superspin Hall effect to disappear for very

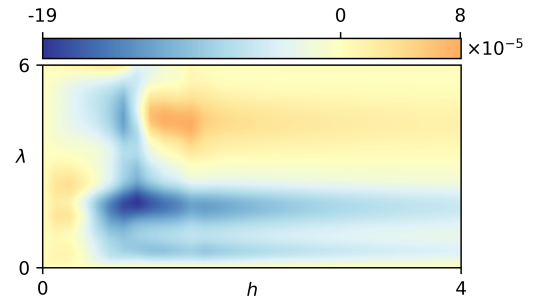


Figure 12. Dependence of the anomalous current $I(0) = \langle I^x \rangle$ on the ferromagnet exchange field h and the Rashba metal spin–orbit coupling λ . Except for h and λ , the parameter values are identical to Fig. 10.

large spin–orbit coupling because it suppresses the necessary p_y -wave spin-0 triplets [41] (\mathbf{d} not parallel to \mathbf{g}_k in the notation of Ref. [81]).

IX. DISCUSSION

The superspin Hall effect and its inverse depend on the existence of p -wave correlations in the junction. These correlations are sensitive to disorder and will, in the face of too large amounts of disorder, be entirely suppressed.

The suppression of superconductivity by disorder has been studied in many systems, including heavy-fermion systems [82, 83], iron pnictides [84, 85], and Sr_2RuO_4 [86]. Strontium ruthenate is arguably the most relevant system for the p -wave correlations that the superspin Hall effect depends on. In strontium ruthenate, the disorder-dependence of the critical temperature can be described using Abrikosov–Gor’kov pair-breaking theory [3, 87]. Superconductivity vanishes in this compound when the mean-free path ℓ is on the order of or smaller than the superconducting coherence length ξ of the p -wave order parameter. Experiments indicate that this corresponds to a residual resistivity of about $1\,\mu\Omega\,\text{cm}$ [86]. Results from the iron pnictides indicates that s_{\pm} -wave pairing is suppressed at a similar residual resistivity of about $10\,\mu\Omega\,\text{cm}$ [85], corresponding to an impurity concentration of only about 1 % [84].

We expect that a similar strong suppression of the p -wave correlations will take place in the junctions we consider. To realize the effects we predict experimentally would thus require samples with good crystallinity and impurity concentrations below about 1 %.

In the weakly disordered case—that is, for impurity concentrations below this level—we expect that the amount of p -wave correlations will be reduced, but not have vanished completely. This will lead to a reduction in the induced transverse spin current (superspin Hall effect) or the induced anomalous current (inverse superspin Hall effect) compared to the clean limit. For comparison, it is instructive to compare the behavior in this case to Fig. 12. Here, the p_y -wave spin-0 triplets are suppressed at large spin–orbit coupling, and the anomalous current vanishes. Similar behavior can be expected as a function of impurity concentration.

X. CONCLUSION

We have considered the superspin Hall and the inverse superspin Hall effects in a two-dimensional S/N/F/N/S Josephson junction. We present two main results.

Firstly, the transverse spin supercurrent induced by the superspin Hall effect circulates from the N/F/N spacer, into the superconductors, and back into the N/F/N spacer. Consequently, it does not give rise to a spin magnetization at the sample edges, contrary to the usual spin Hall effect. The spin magnetization that *does* arise at the sample edges can be attributed to interaction between the proximity-induced even-frequency s -wave spin-singlet condensate and odd-frequency s -wave spin-triplet correlations.

Secondly, we predict and numerically confirm the existence of the inverse superspin Hall effect, which can be detected experimentally as a ϕ_0 shift in the Josephson junction. We have shown that both exchange spin currents and spin-polarized charge supercurrents produce a transverse charge supercurrent by the inverse superspin Hall effect. In particular, we propose that a ϕ_0 junction produced by the inverse superspin Hall effect can be used to—for the first time—measure directly the spin polarization of a charge supercurrent carried by triplet Cooper pairs.

ACKNOWLEDGMENTS

We would like to thank M. Amundsen and J. A. Ouassou for useful discussions. Funding via the “Outstanding Academic Fellows” program at NTNU, the NV Faculty, the Research Council of Norway Grant No. 240806, and the Research Council of Norway through its Centres of Excellence funding scheme, Project No. 262633, “QuSpin” is gratefully acknowledged. This research has benefited from the Notur high-performance computing facilities, Project No. NN9577K.

-
- [1] J. Linder and J. W. A. Robinson, “Superconducting spintronics,” *Nature Physics* **11**, 307–315 (2015).
 - [2] M. Tinkham, *Introduction to Superconductivity*, 2nd ed. (McGraw-Hill, 1996).
 - [3] P. G. de Gennes, *Superconductivity of Metals and Alloys*, Advanced Book Classics (Westview Press, 1999).
 - [4] K. Fossheim and A. Sudbø, *Superconductivity: Physics and Applications* (John Wiley & Sons, 2004).
 - [5] M. Eschrig and T. Löfwander, “Triplet supercurrents in clean and disordered half-metallic ferromagnets,” *Nature Physics* **4**, 138–143 (2008).
 - [6] M. Eschrig, “Spin-polarized supercurrents for spintronics,” *Physics Today* **64**, 43 (2011).
 - [7] M. Eschrig, “Spin-polarized supercurrents for spintronics: A review of current progress,” *Reports on Progress in Physics* **78**, 104501 (2015).
 - [8] P. Fulde and R. A. Ferrell, “Superconductivity in a strong spin-exchange field,” *Physical Review* **135**, A550–A563 (1964).
 - [9] A. I. Larkin and Yu. N. Ovchinnikov, “Inhomogeneous state of superconductors,” *Soviet Physics JETP* **20**, 762 (1965).
 - [10] F. S. Bergeret, A. F. Volkov, and K. B. Efetov, “Long-range proximity effects in superconductor-ferromagnet structures,” *Physical Review Letters* **86**, 4096–4099 (2001).
 - [11] F. S. Bergeret, A. F. Volkov, and K. B. Efetov, “Odd triplet

- superconductivity and related phenomena in superconductor-ferromagnet structures,” *Reviews of Modern Physics* **77**, 1321–1373 (2005).
- [12] A. I. Buzdin, “Proximity effects in superconductor-ferromagnet heterostructures,” *Reviews of Modern Physics* **77**, 935–976 (2005).
- [13] F. S. Bergeret and I. V. Tokatly, “Singlet-triplet conversion and the long-range proximity effect in superconductor-ferromagnet structures with generic spin dependent fields,” *Physical Review Letters* **110**, 117003 (2013).
- [14] F. S. Bergeret and I. V. Tokatly, “Spin-orbit coupling as a source of long-range triplet proximity effect in superconductor-ferromagnet hybrid structures,” *Physical Review B* **89**, 134517 (2014).
- [15] V. P. Mineev and G. E. Volovik, “Electric dipole moment and spin supercurrent in superfluid ^3He ,” *Journal of Low Temperature Physics* **89**, 823–830 (1992).
- [16] F. Meier and D. Loss, “Magnetization transport and quantized spin conductance,” *Physical Review Letters* **90**, 167204 (2003).
- [17] E. B. Sonin, “Spin currents and spin superfluidity,” *Advances in Physics* **59**, 181–255 (2010).
- [18] E. B. Sonin, “Proposal for measuring mechanically equilibrium spin currents in the Rashba medium,” *Physical Review Letters* **99**, 266602 (2007).
- [19] I. Kulagina and J. Linder, “Spin supercurrent, magnetization dynamics, and φ -state in spin-textured Josephson junctions,” *Physical Review B* **90**, 054504 (2014).
- [20] I. V. Bobkova, A. M. Bobkov, and M. A. Silaev, “Spin torques and magnetic texture dynamics driven by the supercurrent in superconductor/ferromagnet structures,” *Physical Review B* **98**, 014521 (2018).
- [21] J. Sinova, S. O. Valenzuela, J. Wunderlich, C. H. Back, and T. Jungwirth, “Spin Hall effects,” *Reviews of Modern Physics* **87**, 1213–1260 (2015).
- [22] L. Onsager, “Reciprocal relations in irreversible processes. I,” *Physical Review* **37**, 405–426 (1931).
- [23] L. Onsager, “Reciprocal relations in irreversible processes. II,” *Physical Review* **38**, 2265–2279 (1931).
- [24] S. R. de Groot, *Thermodynamics of Irreversible Processes*, Selected Topics in Modern Physics, Vol. 3 (North-Holland Publishing Company, 1951).
- [25] E. Saitoh, M. Ueda, H. Miyajima, and G. Tatara, “Conversion of spin current into charge current at room temperature: Inverse spin-Hall effect,” *Applied Physics Letters* **88**, 182509 (2006).
- [26] K. Uchida, S. Takahashi, K. Harii, J. Ieda, W. Koshibae, K. Ando, S. Maekawa, and E. Saitoh, “Observation of the spin Seebeck effect,” *Nature* **455**, 778–781 (2008).
- [27] S. Y. Huang, X. Fan, D. Qu, Y. P. Chen, W. G. Wang, J. Wu, T. Y. Chen, J. Q. Xiao, and C. L. Chien, “Transport magnetic proximity effects in platinum,” *Physical Review Letters* **109**, 107204 (2012).
- [28] M. Weiler, M. Althammer, Franz D. Czeschka, H. Huebl, M. S. Wagner, M. Opel, I.-M. Imort, G. Reiss, A. Thomas, R. Gross, and S. T. B. Goennenwein, “Local charge and spin currents in magnetothermal landscapes,” *Physical Review Letters* **108**, 106602 (2012).
- [29] K. Ando, S. Takahashi, K. Harii, K. Sasage, J. Ieda, S. Maekawa, and E. Saitoh, “Electric manipulation of spin relaxation using the spin Hall effect,” *Physical Review Letters* **101**, 036601 (2008).
- [30] H. Kontani, J. Goryo, and D. S. Hirashima, “Intrinsic spin Hall effect in the s -wave superconducting state: Analysis of the Rashba model,” *Physical Review Letters* **102**, 086602 (2009).
- [31] A. G. Mal’shukov and C. S. Chu, “Spin-Hall current and spin polarization in an electrically biased SNS Josephson junction,” *Physical Review B* **84**, 054520 (2011).
- [32] S. Pandey, H. Kontani, D. S. Hirashima, R. Arita, and H. Aoki, “Spin Hall effect in iron-based superconductors: A Dirac-point effect,” *Physical Review B* **86**, 060507(R) (2012).
- [33] A. G. Mal’shukov, “Supercurrent generation by spin injection in an s -wave superconductor–Rashba metal bilayer,” *Physical Review B* **95**, 064517 (2017).
- [34] C. Espedal, P. Lange, S. Sadjina, A. G. Mal’shukov, and A. Brataas, “Spin Hall effect and spin swapping in diffusive superconductors,” *Physical Review B* **95**, 054509 (2017).
- [35] T. Wakamura, H. Akaike, Y. Omori, Y. Niimi, S. Takahashi, A. Fujimaki, S. Maekawa, and Y. Otani, “Quasiparticle-mediated spin Hall effect in a superconductor,” *Nature Materials* **14**, 675–678 (2015).
- [36] K. Sengupta, R. Roy, and M. Maiti, “Spin Hall effect in triplet chiral superconductors and graphene,” *Physical Review B* **74**, 094505 (2006).
- [37] A. G. Mal’shukov, S. Sadjina, and A. Brataas, “Inverse spin Hall effect in superconductor/normal-metal/superconductor Josephson junctions,” *Physical Review B* **81**, 060502(R) (2010).
- [38] F. S. Bergeret and I. V. Tokatly, “Manifestation of extrinsic spin hall effect in superconducting structures: Nondissipative magnetoelectric effects,” *Physical Review B* **94**, 180502(R) (2016).
- [39] A. G. Mal’shukov and C. S. Chu, “Spin Hall effect in a Josephson contact,” *Physical Review B* **78**, 104503 (2008).
- [40] Z.-H. Yang, Y.-H. Yang, and J. Wang, “Interfacial spin Hall current in a Josephson junction with Rashba spin–orbit coupling,” *Chinese Physics B* **21**, 057402 (2012).
- [41] J. Linder, M. Amundsen, and V. Risinggård, “Intrinsic superspin Hall current,” *Physical Review B* **96**, 094512 (2017).
- [42] F. Konschelle, I. V. Tokatly, and F. S. Bergeret, “Theory of the spin-galvanic effect and the anomalous phase shift φ_0 in superconductors and Josephson junctions with intrinsic spin-orbit coupling,” *Physical Review B* **92**, 125443 (2015).
- [43] R. S. Keizer, S. T. B. Goennenwein, T. M. Klapwijk, G. Miao, G. Xiao, and A. Gupta, “A spin triplet supercurrent through the half-metallic ferromagnet CrO_2 ,” *Nature* **439**, 825–827 (2006).
- [44] T. S. Khaire, M. A. Khasawneh, W. P. Pratt, and N. O. Birge, “Observation of spin-triplet superconductivity in Co-based Josephson junctions,” *Physical Review Letters* **104**, 137002 (2010).
- [45] J. W. A. Robinson, J. D. S. Witt, and M. G. Blamire, “Controlled injection of spin-triplet supercurrents into a strong ferromagnet,” *Science* **329**, 59–61 (2010).
- [46] M. S. Anwar, M. Veldhorst, A. Brinkman, and J. Aarts, “Long range supercurrents in ferromagnetic CrO_2 using a multilayer contact structure,” *Applied Physics Letters* **100**, 052602 (2012).
- [47] W. M. Martinez, W. P. Pratt, and N. O. Birge, “Amplitude control of the spin-triplet supercurrent in S/F/S Josephson junctions,” *Physical Review Letters* **116**, 077001 (2016).
- [48] A. Singh, C. Jansen, K. Lahabi, and J. Aarts, “High-quality CrO_2 nanowires for dissipation-less spintronics,” *Physical Review X* **6**, 041012 (2016).
- [49] J. C. Slonczewski, “Conductance and exchange coupling of two ferromagnets separated by a tunneling barrier,” *Physical Review B* **39**, 6995–7002 (1989).
- [50] W. Chen, P. Horsch, and D. Manske, “Dissipationless spin current between two coupled ferromagnets,” *Physical Review B* **89**, 064427 (2014).
- [51] Y. Tanaka, A. A. Golubov, S. Kashiwaya, and M. Ueda, “Anomalous Josephson effect between even- and odd-frequency superconductors,” *Physical Review Letters* **99**, 037005 (2007).
- [52] M. Eschrig, T. Löfwander, T. Champel, J. C. Cuevas, J. Kopu, and G. Schön, “Symmetries of pairing correlations in superconductor–ferromagnet nanostructures,” *Journal of Low Temperature*

- Physics* **147**, 457–476 (2007).
- [53] M. Sigrist and K. Ueda, “Phenomenological theory of unconventional superconductivity,” *Reviews of Modern Physics* **63**, 239–311 (1991).
 - [54] D. S. Dummit and R. M. Foote, *Abstract Algebra*, 3rd ed. (John Wiley & Sons, 2004).
 - [55] F. R. Gantmacher, *The Theory of Matrices*, Vol. 1 (American Mathematical Society, 2000).
 - [56] J. A. Ouassou, S. H. Jacobsen, and J. Linder, “Conservation of spin supercurrents in superconductors,” *Physical Review B* **96**, 094505 (2017).
 - [57] A. J. Leggett, “A theoretical description of the new phases of liquid ^3He ,” *Reviews of Modern Physics* **47**, 331–414 (1975).
 - [58] J. M. D. Coey, *Magnetism and Magnetic Materials* (Cambridge University Press, 2010).
 - [59] R. C. O’Handley, *Modern Magnetic Materials: Principles and Applications* (John Wiley & Sons, 2000).
 - [60] J.-F. Liu and K. S. Chan, “Relation between symmetry breaking and the anomalous Josephson effect,” *Physical Review B* **82**, 125305 (2010).
 - [61] J.-F. Liu and K. S. Chan, “Anomalous Josephson current through a ferromagnetic trilayer junction,” *Physical Review B* **82**, 184533 (2010).
 - [62] D. B. Szombati, S. Nadj-Perge, D. Car, S. R. Plissard, E. P. A. M. Bakkers, and L. P. Kouwenhoven, “Josephson φ_0 -junction in nanowire quantum dots,” *Nature Physics* **12**, 568–572 (2016).
 - [63] A. Rasmussen, J. Danon, H. Suominen, F. Nichele, M. Kjaergaard, and K. Flensberg, “Effects of spin-orbit coupling and spatial symmetries on the Josephson current in SNS junctions,” *Physical Review B* **93**, 155406 (2016).
 - [64] V. Chandrasekhar, “Proximity-coupled systems: quasiclassical theory of superconductivity,” in *Superconductivity*, edited by K. H. Bennemann and J. B. Ketterson (Springer, 2008) pp. 279–313.
 - [65] A. M. Black-Schaffer and J. Linder, “Strongly anharmonic current-phase relation in ballistic graphene Josephson junctions,” *Physical Review B* **82**, 184522 (2010).
 - [66] C. D. English, D. R. Hamilton, C. Chialvo, I. C. Moraru, N. Mason, and D. J. Van Harlingen, “Observation of nonsinusoidal current-phase relation in graphene Josephson junctions,” *Physical Review B* **94**, 115435 (2016).
 - [67] Y. K. Kato, R. C. Myers, A. C. Gossard, and D. D. Awschalom, “Observation of the spin Hall effect in semiconductors,” *Science* **306**, 1910–1913 (2004).
 - [68] J. Wunderlich, B. Kaestner, J. Sinova, and T. Jungwirth, “Experimental observation of the spin-Hall effect in a two-dimensional spin-orbit coupled semiconductor system,” *Physical Review Letters* **94**, 047204 (2005).
 - [69] K. Halterman, O. T. Valls, and P. H. Barsic, “Induced triplet pairing in clean s -wave superconductor/ferromagnet layered structures,” *Physical Review B* **77**, 174511 (2008).
 - [70] D. Terrade, D. Manske, and M. Cuoco, “Control of edge currents at a ferromagnet–triplet superconductor interface by multiple helical modes,” *Physical Review B* **93**, 104523 (2016).
 - [71] Shin-ichi Hikino, “Magnetization reversal by tuning Rashba spin–orbit interaction and Josephson phase in a ferromagnetic Josephson junction,” *Journal of the Physical Society of Japan* **87**, 074707 (2018).
 - [72] A. F. Andreev, “The thermal conductivity of the intermediate state in superconductors,” *Soviet Physics JETP* **19**, 1228 (1964).
 - [73] J. A. Sauls, “Andreev bound states and their signatures,” *Philosophical Transactions of the Royal Society A: Mathematical, Physical and Engineering Sciences* **376**, 20180140 (2018).
 - [74] I. Kulik and A. Omelyanchuk, “Properties of superconducting microbridges in the pure limit,” *Soviet Journal of Low Temperature Physics* **3**, 459–461 (1977).
 - [75] J. Linder, T. Yokoyama, D. Huertas-Hernando, and A. Sudbø, “Supercurrent switch in graphene π junctions,” *Physical Review Letters* **100**, 187004 (2008).
 - [76] Note that the term *inverse effect* cannot here be understood as the Onsager reciprocal proper, as our calculations are carried out in *equilibrium*.
 - [77] A. A. Golubov, M. Yu. Kupriyanov, and E. Il’ichev, “The current-phase relation in Josephson junctions,” *Reviews of Modern Physics* **76**, 411–469 (2004).
 - [78] J. A. Ouassou and J. Linder, “Voltage control of superconducting exchange interaction and anomalous Josephson effect,” [arXiv:1810.02820](https://arxiv.org/abs/1810.02820).
 - [79] J. A. Glick, V. Aguilar, A. B. Gougam, B. M. Niedzielski, Eric C. Gingrich, R. Loloee, W. P. Pratt, and N. O. Birge, “Phase control in a spin-triplet SQUID,” *Science Advances* **4**, eaat9457 (2018).
 - [80] N. W. Ashcroft and N. D. Mermin, *Solid State Physics*, 1st ed. (Harcourt College Publishers, 1976).
 - [81] P. A. Frigeri, D. F. Agterberg, A. Koga, and M. Sigrist, “Superconductivity without inversion symmetry: MnSi versus CePt $_3$ Si,” *Physical Review Letters* **92**, 097001 (2004).
 - [82] Y. Dalichaouch, M. C. de Andrade, D. A. Gajewski, R. Chau, P. Visani, and M. B. Maple, “Impurity scattering and triplet superconductivity in UPt $_3$,” *Physical Review Letters* **75**, 3938–3941 (1995).
 - [83] C. Geibel, C. Schank, F. Jähring, B. Buschinger, A. Grauel, T. Lühmann, P. Gegenwart, R. Helfrich, P.H.P. Reinders, and F. Steglich, “Doping effects on UPd $_2$ Al $_3$,” *Physica B: Condensed Matter* **199–200**, 128–131 (1994).
 - [84] Seiichiro Onari and Hiroshi Kontani, “Violation of Anderson’s theorem for the sign-reversing s -wave state of iron-pnictide superconductors,” *Physical Review Letters* **103**, 177001 (2009).
 - [85] Y. Wang, A. Kreisel, P. J. Hirschfeld, and V. Mishra, “Using controlled disorder to distinguish s_{\pm} and s_{++} gap structure in Fe-based superconductors,” *Physical Review B* **87**, 094504 (2013).
 - [86] A. P. Mackenzie, R. K. W. Haselwimmer, A. W. Tyler, G. G. Lonzarich, Y. Mori, S. Nishizaki, and Y. Maeno, “Extremely strong dependence of superconductivity on disorder in Sr $_2$ RuO $_4$,” *Physical Review Letters* **80**, 161–164 (1998).
 - [87] A. A. Abrikosov and L. P. Gor’kov, “Contribution to the theory of superconducting alloys with paramagnetic impurities,” *Soviet Physics—JETP* **12**, 1243 (1961).